Arterial Input Function segmentation based on a contour geodesic model for tissue at risk identification in Ischemic Stroke

1.Sukhdeep Singh Bal

Department of Mathematical sciences, University of Liverpool, Liverpool, UK.
Center for Cognition and Mind Sciences, National Tsing Hua University, Taiwan.
International Intercollegiate Ph.D. Programme, National Tsing Hua University, Taiwan.
email: sukhdeep.singh.bal.@liverpool.ac.uk, sukhdeepsinghbal2016@gmail.com

2. Ke Chen, Ph.D

Department of Mathematical sciences, University of Liverpool, Liverpool, Merseyside, UK.
email: K.Chen@liverpool.ac.uk

3. Fan Pei Gloria Yang*, Ph.D. (Corresponding Author)

Department of Foreign Languages and Literature, National Tsing Hua University, Taiwan.
Center for Cognition and Mind Sciences, National Tsing Hua University, Taiwan.
Department of Radiology, Graduate School of Dentistry, Osaka University, Japan.
No. 101, Section 2, Guangfu Road, East District, Hsinchu City, Taiwan 300.
email: hbmyang@gmail.com

4. Dr. Giia-Sheun Peng

Department of Neurology, Tri-Service General Hospital, National Defense Medical Center, Taipei, Taiwan.
Division of Neurology, Department of Internal Medicine, Taipei Veterans General Hospital, Hsinchu Branch, Hsinchu County, Taiwan.
email: tsghpeng@gmail.com

Running title : Arterial Input Function segmentation

Author to whom correspondence should be addressed. email: hbmyang@gmail.com

This article has been accepted for publication and undergone full peer review but has not been through the copyediting, typesetting, pagination and proofreading process, which may lead to differences between this version and the Version of Record. Please cite this article as doi: 10.1002/mp.15508

Abstract

Purpose: Perfusion parameters such as cerebral blood flow (CBF) and Tmax have been proven to be useful in the diagnosis and prognosis for Ischemic stroke. Arterial input function (AIF) is required as an input to estimate perfusion parameters. This makes the AIF selection paradigm of clinical importance.
Methods: This study proposes a new technique to address the problem of AIF selection, based on a variational segmentation model that combines geometric constraint in a distance function. The modified model uses discrete total variation in the distance term and via minimizing an energy locates the arterial regions. Matrix analysis is utilized to identify the AIF with maximum peak height within the segmented region.
Results: Group mean differences indicate that overall the AIF selected by purposed method has better arterial features of higher peak position (16.7 a.u and 26.1 a.u) and fast attenuation (1.08 seconds and .9 seconds) as compared to the other state of the art methods. Utilizing the selected AIF, mean CBF and Tmax values were estimated higher than the traditional methods. Ischemic regions were precisely located through the perfusion maps.
Conclusions: This AIF segmentation framework worked on perfusion images at levels superior to the current clinical state of the art. Consequently, the perfusion parameters derived from AIF selected by the purposed method were more accurate and reliable. The proposed method could potentially be considered as part of the calculation for perfusion imaging in general.

keywords : Cerebral perfusion imaging, dynamic susceptibility contrast, cerebral blood flow, variation model, AIF measurements.

I. Introduction

Ischemic stroke may result in dysfunctions, disorders and death[1]. Diagnosis and treatment of stroke rely on accurate measurement of cerebral perfusion done after the injection of MR paramagnetic contrast agent[2,3,4]. Cerebral perfusion refers to rate of blood delivery to the brain tissues[4]. Among different MRI methods Dynamic Susceptibility Contrast (DSC) MRI perfusion imaging method is preferred for diagnosis due to the features of fast acquisition time and optimal contrast-to-noise ratio[4,5]. Perfusion model based on indicator dilution theory is fitted on the information obtained from perfusion data sets to obtain certain perfusion parameters as an output result[3,4,6]. Output from PWI include the Cerebral blood flow (CBF), cerebral blood volume, perfusion-diffusion mismatch, which are used to identify the infarct core and tissue at risk or the penumbra[7].

DSC perfusion data sets posses the information of concentration of contrast agent present in the brain tissues in the form of concentration -time curves[2,6,8]. According to the perfusion model concentration -time curves are considered as a convolution of the response function with the Arterial Input Function (AIF), which is the concentration of the contrast agent over time in a brain-feeding artery[8]. To analyze blood flow in the ischemic tissue, deconvolution of concentration -time curves with the AIF is necessary. The AIF is a key reference curve used in the deconvolution model to obtain quantitative CBF, CBV and perfusion-diffusion mismatch estimation. Selection of the AIF curve influences the result of the deconvolution operation and this makes AIF a key aspect of CBF quantification using DSC MRI[4,9].

There has been plenty of progress in recent years regarding how and where to measure AIF[4]. Although the AIF should, in principle, be measured from inside an artery (or at least from a voxel that contains primarily arterial contributions), but many studies in past often considered measuring the AIF from the region outside or from a region in the vicinity of an artery[4]. Also, from a practical point of view, due to the coarse spatial resolution of DSC- (the typical voxel size is 2x2x5 mm3) it is difficult to measure the signal from inside a small artery[10]. Usually in MR-PWI studies suitable AIF voxels are chosen by inspecting the peak shape characteristics (e.g., arrival time, height, width, etc.) in a region in and around

arteries. The name given to this input function is generally Arterial Input function (AIF).

To improve reliability, quality, and reproducibility of the AIF selection several automatic and semiautomatic methods have been proposed[3,10,11,12]. The majority of the toolboxes pre-installed in MR scanners use either manual, clustering or arterial likelihood methods for AIF estimation. For manual AIF selection, a trained clinical operator based on his experience and judgement selects a small number of pixels containing region of one of the principal arterial vessels[13]. Manual location of AIF is not preferred as this reduces the procedure reproducibility[10]. Low spatial resolution of MR-PWI data also makes manual selection difficult on contrast-MRI-PWI images[3,11].

Automatic methods were developed to overcome the shortcomings of the manual AIF selection procedure[3,12,13]. The clustering based method uses the middle cerebral artery (MCA) as a elliptical region of interest (ROI) and then utilizes a recursive cluster analysis to select the arterial voxels[3]. Inefficient AIF selection usually occurs in the cases where the elliptical ROI does not segment the MCA precisely and some of the arterial voxels are left on the boundary or in the vicinity of the elliptical marker.

Some softwares use arterial likelihood methods so as to select the potential AIF to match the arterial features[11]. This includes minimizing the bolus arrival time, peak width and maximize the peak height. AIF detection algorithm searches for locations or voxels with signals of above-average amplitude or height along with below-average width and early bolus-arrival time using a cost function. Final AIF locations are selected in a region with the highest sum of the clustered values of cost function. Incorrect or flawed selection in this method arises from the weighting factors used as the penalty factor used for peak height is much lower than the other penalty factors used in calculation of cost function. This results in selection of an AIF voxel with a shallow or low peak height. Apart from these methods several studies use different approaches, like a local AIF extraction method was introduced to replace the global AIF[9,14,15]. Despite of the presence of multiple studies to select AIF, in this study we mainly focus to use to a model to select a AIF with higher amplitude and early time to peak.

To overcome the limitation of past methods, we purpose an improved convex segmentation model. The PWI images are usually of low contrast which makes detection of edges difficult[4]. To solve this problem we use a new idea of discrete Total Variation (TV) in a convex geodesic model. This TV helps in locating the boundary of arterial regions to separate homogeneous regions or intensity jumps[16]. The modified segmentation model via minimizing an energy can locate the arterial regions more accurately. After segmenting the arterial region, we use matrix analysis to find the voxel with maximum peak height within the contour to overcome the problem associated with shallow or low peak height AIF selection. Furthermore, to demonstrate better accuracy and arterial features obtained by the proposed model, a statistical comparison based on PWI dataset of 15 patients is made between the present method and the previous methods.

II. Methods

In the proposed method, we focus on the selective segmentation or specifying the location of the potential voxels which could be used as AIF in the vicinity of an artery. Initially a contour representing a region of interest (ROI) is drawn in the surrounding of the arterial location (Figure 1). For this purpose, convex based geodesic selective model is used to draw the contour on the middle slice of the brain axial images[17]. The advantage with a contour-based selective segmentation is exclusion of the CSF region as the contour model segments the ROI region based on homogeneous intensity values. After the segmentation of the ROI, the matrix analysis is used to find the potential voxel with maximum peak height within the contour (Figure 1). This ensures that the location or pixel with maximum height within the contour is selected as the potential AIF.

II.A. Proposed contour based AIF Segmentation method

The energy functional of convex geodesic selective model differs from initial segmentation models as it includes intensity fitting terms as well as distance penalty term which uses geodesic distance from the marker set rather than the Euclidean distance[17,18,19]. Here, we utilise a Total Variation function in the distance term of the model for denoising the image (cf.[16] for more information on the Discrete TV utilised in the model). The contour model

involves a convex function and is to be minimized to achieve segmentation. The minimizer of this function specifies the criteria to segment selective objects. The minimizer of the function is in the form of partial differential equation. The definition of the function is -

Let $z(x,y)$ represent the input PWI image, defined on a image domain $\Omega \subset R^2$. u represents the level set of initial contour . c_1, c_2 are average intensities of z inside and outside u. The functional is in the following form-

$$F_(u,c_1,c_2) = \mu \int_\Omega g(|\nabla z(x,y)|)|\nabla u| d\Omega +$$

$$\int_\Omega [\lambda_1(z(x,y)-c_1)^2 - \lambda_2(z(x,y)-c_2)^2]ud\Omega + \theta \int_\Omega D_M(x,y)ud\Omega + \alpha \int_\Omega \nu_\epsilon(u)d\Omega \quad (1)$$

(1)

θ,μ,λ_1, λ_2 are non negative parameters. The term $g(|\nabla z|)$ is the edge detector which is $g(s) = 1/1+\beta s^2$ where β is tuning parameter. The last term is an exact penalty term due to convex formulation of the functional, where $v(u)= max\{0, 2|u-\frac{1}{2}|-1\}$. This is done to achieve unconstrained minimization as this encourages the minimizer to be in range [0,1]. We refer the reader to[17,18,20] for more information on the model. Next we illustrate the calculation of Geodesic term D_M.[17].

The geodesic distance from the marker set M is given by $D_M(x,y) = 0$ for $(x,y) \in M$ and $D_M(x,y) = \frac{D^0_M(x,y)}{||D^0_M||_{L\infty}}$ for $(x,y) \notin M$, where $D^0_M(x,y)$ is the solution of the following PDE:

$$|\nabla D^0_M(x,y)| = f(x,y), D^0_M(x0,y0) = 0, (x0,y0) \in M. \quad (2)$$

To improve noise robustness and qualitative nature of segmentation results, we considered TV denoising by utilising the new definition of TV. The formulation of the discrete TV to

be used in the geodesic term is[16] -

$$TV_p(x) = min\{||v_{\updownarrow}||_{1,2} + ||v_{\leftrightarrow}||_{1,2} + ||v_{.}||_{1,2} : L^*_{\updownarrow}v_{\updownarrow} + L^*_{\leftrightarrow}v_{\leftrightarrow} + L^*_{.}v_{.} = Dx\} \quad (3)$$

Here, v is the whole gradient field, which is the concatenation of $v_{\updownarrow}, v_{\leftrightarrow}, v_{.}$ vector fields solution to above equation. Its elements $v_{\updownarrow}(n_1, n_2), v_{\leftrightarrow}(n_1, n_2), v_{.}(n_1, n_2)$ are vectors located at positions $(n_1 + \frac{1}{2}, n_2), (n_1, n_2 + \frac{1}{2}), (n_1, n_2)$. The proposed TV is the $l_{1,2}$ norm of the gradient field v associated to the image x, defined on a grid three times more dense than the one of x[16]. Defining it on a three times finer grid allow this TV to detect edges in low contrast regions, when used in segmentation model (cf.[16] for more information). The new f is formulated as -

$$f(x, y) = \epsilon_D + \beta_G|\nabla S_p(z(x, y))|^2 + \nu D_E(x, y) \quad (4)$$

Here $\nabla S_p\ z(x, y)$ represents the gradient field achieved after denoising is done with the new purposed TV and D_E is the euclidean distance. We use calculus of variation and solve above equation (1) with respect to c_1 and c_2 with u fixed (cf.[18] for more information on solving the equation). This leads to-

$$c_1(u) = \frac{\int_\Omega u.z(x, y))d\Omega}{\int_\Omega u d\Omega} \quad (5)$$

$$c_2(u) = \frac{\int_\Omega (1 - u).z(x, y))d\Omega}{\int_\Omega (1 - u)d\Omega} \quad (6)$$

Using calculus of variation and solving above equation with respect to u with fixed c_1 and c_2 leads to Euler's equation[18,20]

$$\mu\nabla(g(|\nabla z(x, y)|)\frac{\nabla u}{|\nabla u|_{\epsilon_2}}) - [\lambda_1(z(x, y) - c_1)^2 - \lambda_2(z(x, y) - c_2)^2] - \theta D_G(x, y) - \alpha\nu'_\epsilon(u) = 0 \quad (7)$$

We also have Neumann boundary conditions $\frac{\delta u}{\delta n} = 0$ on $\delta\Omega$ where n is the outward unit normal vector. The Numerical solution of the above equation decides the contour that segments the Arterial region (cf.[17,21] for information on the numerical solution and the scheme used).

II.B. Purposed Matrix analysis to find the potential AIF within the contour

Matrix analysis was utilized to select the potential AIF voxels out of all the voxels in the contour. The steps used to select appropriate voxels inside the segmented region were as following-

1) The coordinates (i, j) of segmented region inside contour represented by u were formed into a array A.

$$A = \begin{pmatrix}(i_1, j_1) & (i_2 & j_2) & ...(i_n, j_n)\end{pmatrix}^T \tag{8}$$

2) Matrix C had the information of concentration of contrast agent at each (x, y, z, t) of the brain images, where x, y were location of coordinates in brain image, z was the slice selected for AIF extraction and t represented time points.

$$C = (x, y, z, t) \tag{9}$$

3) For the the n segmented (i,j) coordinates in the A array, we form following $1 \times n$ row vector C_1,C_2,..C_k at different time points k.

$$C_k = \begin{pmatrix}Conc(i_1, j_1, z, k) & Conc(i_2, j_2, z, k) & .....Conc(i_n, j_n, z, k)\end{pmatrix} \tag{10}$$

This is done to form a final $k \times n$ concentration matrix F which represents information of concentration of contrast agent in all the selected voxels inside contour at different time point in a row wise manner.

$$F = \begin{pmatrix}C_1 & C_2 & ..C_k\end{pmatrix}^T \tag{11}$$

4) Maximum of F matrix will be the highest amplitude of concentration curves among all time points and all the voxels. This purposed analysis is used to trace back the spatial location of the best potential AIF voxels. Finally, global AIF for perfusion analysis is represented by the contrast agent concentration of the selected AIF voxel.

II.C. Perfusion Data acquisition

During the diagnostic MR procedure, fifteen ischemic stroke patients underwent perfusion imaging. A clinical 1.5 T MR scanner at the Tri-service General Hospital, Taipei (Signa; General Electric) was used to acquire contrast-enhanced T2*-weighted images. Single-shot gradient-echo EPI sequence was utilised (TR : 1800 ms, TE : 40 ms). During Perfusion imaging, bolus injection (Magnevist; gadopentetate dimeglumine, Bayer Health Care pharmaceuticals Inc.) was injected with the speed of 5 ml/sec and quantity was 20 ml. After the contrast agent passes through the tissues, the decrease in signal intensity depends on the contrast agent concentration, which is considered as a proxy for perfusion. The acquired time series data are then postprocessed to obtain perfusion maps with different parameters. The additional benefit of using this type of dataset is to accentuate local magnetic homogeneity effects to aid in the detection of hemorrhage, core and better segmentation[22]. This study was granted IRB approval from the Tri-Service General Hospital, Taipei, Taiwan.

II.D. Statistical analysis and Perfusion parameter estimation

Statistical analysis

AIF location on the brain axial slices was decided by utilising different methods: clustering method, arterial likelihood method and contour based AIF segmentation method. Due to the different patient conditions, physical condition, severity of the disease, the contrast injection time, and due to variable time to start the scan, statistical comparisons are only made by using the differences of the curve parameters[10]. These curve parameters are amplitude (peak), the center position of the peak of concentration curve or time to peak, the differences are represented by Δ amplitude (a.u), Δ center (sec). One-way ANOVA statistical test was used to establish whether there is a significant difference in terms of amplitude of AIF selected by the different three methods.

Perfusion Parameter estimation

Perfusion DSC model was used to compute the Perfusion parameters (CBF and Tmax) with the global AIFs deduced from different methods: clustering method, arterial likelihood

method and contour based AIF segmentation method. Perfusion analysis was done once global AIF was decided by the AIF selection methods. On the lines on past perfusion studies in ischemic stroke, perfusion analysis was done by deconvolution of the tracer kinetic equation[8,23,24,25].

$$C_t = C_a \otimes R(t) \tag{12}$$

All the image analysis were implemented in MATLAB. (Mathworks, Natick, MA). Here $C_t(t)$ denotes the tissue concentration curve at each pixel, $C_a(t)$ is the AIF either using one of the three AIF selection methods described above, symbol $\otimes$ represents the convolution operator and $R(t)$ represents the residue impulse response function. Deconvolution of Eq. [12] to estimate CBF, Tmax was done using the singular value decomposition method (SVD)[8,26,27]. Deconvolution of Eq. [12] for known values of $C_a(t)$, $C_t(t)$ at each pixel of axial slices leads to evaluation of the residue function $R(t)$. CBF is measured as the maximum of $R(t)$[11]. Tmax is the time t for which $R(t)$ attains maximum value[11,25]. After estimating CBF and Tmax for all brain tissues, CBF and Tmax are represented visually on axial slices. Tissue at risk was identified by thresholding the Tmax values by Tmax >6 seconds.

III. Results

III.A. Statistical analysis of Curve Characteristics

Subjectively, the concentration curve of AIF extracted by contour based AIF segmentation method confirmed to the arterial characteristics, such as large amplitude, small width, fast attenuation, and gamma-like shape (Figure 2). In terms of AIF location, it is visible that the location selected by contour based AIF segmentation method is quite close or in proximity of the AIF location selected by arterial likelihood method (Figure 2). In terms of curve characterstics comparison, contour based AIF segmentation method selects AIF curve with larger amplitude or higher peak position and with fast attenuation represented by early time to peak or positive Δ center (Figure 2, Figure 4). We also calculated the similarity of the AIF concentration curves. The similarity was calculated by Correlation Coefficient, which indicates that the curves are positively correlated (Table 1, Table 2, Table 3).

The AIF curve characterstics of all other subjects are represented in the form of statistical tables (Table 1, Table 2). We also show the Group mean differences between the contour based peak height AIF method and the previous AIF selection methods to get a group overview. The group mean differences indicate that overall the AIF selected by contour based AIF segmentation method has better arterial features of higher peak position (Figure 5(a)), and fast attenuation as compared to the other AIF selection methods (Table 3). A one-way ANOVA (Figure 4) revealed that there was a statistically significant difference in AIF amplitude (peak) between the three AIF selection methods ($F(2, 42) = 5.66$, $p = .0067$).

The clustering method and arterial likelihood methods have the same peak for patients 12-15 (Tables 1 and 2). The contour-based method uses a matrix based approach to ensure that out of all the potential AIF voxels in the marked contour the selected AIF voxel has the maximum peak concentration. In subjects 12-15 the other two methods miss out AIF with maximum peak which is a feature of utilizing the matrix analysis post selection of ROI for AIF by contour-based model.

In figure 2 we have shown the cases where the contour method selects AIF with better arterial features i.e., high peak and early time to peak than the latter two methods. In figure 3, both the methods select a similar AIF voxel and this represents that in some cases both arterial likelihood method and contour-based method may yield the same result for AIF i.e. in this case arterial likelihood method may not miss out the peak AIF voxel. In contrast, for all other subjects both the AIF locations are quite close but the arterial likelihood method misses out the location with highest peak (Figure 2). This could be due to the varying physical conditions, severity of the disease, noise associated with signals and the variability of contrast injection time among different patients. Although we processed all the samples, considering the number of samples, we only showed selected AIF location and corresponding concentration curve of three of them. For a patient, the contour method yields an AIF curve after 14 s (seconds). Time taken by the clustering method and arterial likelihood method for the AIF estimation was 9 s and 13 s. (Intel I5/Ram :8gb/ MATLAB 2020(a)).

III.B. Perfusion maps

We derived the Perfusion parameters (CBF, Tmax) corresponding to the AIF given by all three methods in each pixel in each sample. For comparison we used a similar SVD deconvolution method with the optimal standard threshold[26]. The perfusion maps were accessed by an experienced clinical from veterans hospital. Based on the feedback investigators concluded that perfusion parameter maps could be utilised for diagnosis.

The distribution of CBF and Tmax maps based on the AIF selected by all three methods is basically the same, however ischemic regions or tissues at risk can be clearly located through the perfusion maps given by contour based segmentation method (Figure 5, Figure 6). The mean and standard deviation of perfusion parameters (CBF and Tmax) over a cohort of all patients are shown in Table 4. The other two AIF selection methods estimate lower Tmax and higher CBF values, which misleads us in terms of severity of Ischemia and the size of tissue at risk. The mean CBF values obtained by our method are in general lower than those obtained by the other two methods (Figure 5, Table 4). The mean Tmax values obtained by Contour based AIF selection method are higher than those obtained by the other two methods (Table 4). Higher Tmax and lower CBF values reported are due to the early time to peak and the larger peak value of the AIF curve.

With the help of a sample example of a stroke patient we illustrate that tissue at risk was clearly located with improved visual specificity (Figure 6). The clustering based AIF method failed to estimate the tissue at risk in this case (Figure 6). Contour based method estimated the size and volume of tissue at risk similar to the size estimated by a widely used commercial software considered as golden standard for perfusion processing outcome.

IV. Discussion

IV.A. AIF and contour based models

Contour based segmentation models have been widely used for object segmentation in images with noise and in homogeneous intensities[17,28,29]. They are usually based on a functional and the minimizer of this functional decides the accuracy of segmentation[18,20,29]. However,up to date this has not yet been applied for AIF estimation in PWI studies. Experimental and comparison results suggest that the discussed method performs better in terms of AIF estimation as compared to earlier methods. The present method has been proved to be robust to detect voxels with large amplitudes, small width, fast attenuation, and gamma-like shape as potential AIF. The utilization of discrete TV allows the contour model to deal with noisy data sets as well as with in homogeneous intensities.

Recent studies utilized a deep convolutional neural network (CNN) to automatically identify AIFs in computed tomography perfusion (CTP) and perfusion-weighted MRI (PWI) datasets[10,30]. These studies concluded that CNN network models could be potentially viable as the cross-correlation values of manual AIFs with CNN AIFs were observed higher than the AIF decided by the traditional methods[30]. The CNN-derived AIFs for the PWI data-sets showed marginally greater peak heights and early time to peak. CNN models require the choice of ground truth as an input and this ground truth is mainly a manual selected AIF. Here, to provide ground truth user has to inspect each voxel which is inside the Arterial ROI. This might be time consuming and there are high chances of missing a voxel which could represent a AIF with better arterial features. Comparatively, the purposed method is selective and just requires a single click to set a marker point or to localize the Arterial region as region of interest (ROI) and find a suitable AIF voxel.

IV.B. Tissue at risk and limitations

Tissue at risk or Ischemic penumbra denotes the stroke region that is at risk of progressing to infarction but is still salvageable[11,31]. Ischemic penumbra is usually located around an infarct core which represents the infarcted or blocked necrotic tissue[32]. Cerebral perfusion

in terms of parameters is the key information that helps to locate the penumbra around the infract core[10,32,33]. AIF plays a central role in cerebral perfusion estimation. PWI studies proved that AIF measured with a lower amplitude, large width and slow attenuation could produce a four times blood flow overestimation along with inaccurate ischemic penumbra[34]. We could observe that (Figure 6) difference in AIF selection makes a substantial bias in the estimation of ischemic penumbra.

With the help of an example (Figure 6) we demonstrate that the accuracy and visual reliability to identify tissue at risk with our model is promising. Among the three methods, contour-based AIF method has the closest prediction of the tissue at risk in comparison to a commercial software. Detection of ischemic infraction is important because of narrow window of therapeutic efficacy. Inclusion of this fast and efficient AIF selection algorithm presented in this study in clinical settings may optimise the delivery of stroke care. The proposed method could potentially be considered as part of the calculation for perfusion imaging in general.

This study has several limitations. In this study, we used MR-PWI data set of 15 patients. In clinical settings, collecting the data-sets for a broader patient cohort is challenging due to the restricted access to urgent MR-PWI and the contraindications (e.g., uncharacterized metallic foreign bodies) related to MR-PWI acquisition[35]. Recent studies have demonstrated that Computed Tomography perfusion (CTP) can provide information related to treatment decision making at a level similar to MR-PWI[35]. Due to the greater accessibility of CTP, further CTP studies on a large data set with variability of onset of stroke are required to demonstrate the consistency of purposed AIF selection method. Also, it would be worth to see if the proposed model can deal with the noise and in-homogeneity in the CT perfusion images.

V. Conclusion

This study proposed a contour-based segmentation model for estimating AIF curves in brain perfusion images. This segmentation framework worked on perfusion images at levels superior to the current clinical state of the art. The model estimated AIF curves with higher amplitude and early time to peak along with a good performance in identifying the tissue at risk. Inclusion of this improved AIF selection methodology discussed in the study will facilitate prediction and localization of the ischemic penumbra ,which in turn may optimise the delivery of stroke care and surgical pharmaceutical treatments.

Conflict of Interest Statement

The authors have no relevant conflicts of interest to disclose.

Data Availability Statement

The data that supports the findings of the study are available from the corresponding author upon reasonable request.

References

1. Naghavi M, Abajobir AA, Abbafati C, *et al.* Global, regional, and national age-sex specific mortality for 264 causes of death, 1980–2016: a systematic analysis for the Global Burden of Disease Study 2016. *The Lancet.* 2017;390(10100):1151-1210.

2. Calamante F, Gadian DG, Connelly A. Delay and dispersion effects in dynamic susceptibility contrast MRI: Simulations using singular value decomposition. *Magnetic Resonance in Medicine.* 2000;44(3):466-473.

3. Peruzzo D, Bertoldo A, Zanderigo F, Cobelli C. Automatic selection of arterial input function on dynamic contrast-enhanced MR images. *Computer Methods and Programs in Biomedicine.* 2011;104(3):e148-e157.

4. Calamante F. Arterial input function in perfusion MRI: A comprehensive review. *Progress in Nuclear Magnetic Resonance Spectroscopy.* 2013;74:1-32.

5. Rosen B, Belliveau J, Vevea J, Brady T. Perfusion imaging with NMR contrast agents. *Magnetic resonance in medicine.* 1990;14(2):249—265.

6. Straka M, Albers GW, Bammer R. Real-time diffusion-perfusion mismatch analysis in acute stroke. *Journal of Magnetic Resonance Imaging.* 2010;32(5):1024-1037.

7. Albers GW, Thijs VN, Wechsler L, *et al.* Magnetic resonance imaging profiles predict clinical response to early reperfusion: The diffusion and perfusion imaging evaluation for understanding stroke evolution (DEFUSE) study. *Annals of Neurology.* 2006;60(5):508-517.

8. Ostergaard L, Sorensen A, Kwong K, Weisskoff R, Gyldensted C, Rosen B. High resolution measurement of cerebral blood flow using intravascular tracer bolus passages. Part II: Experimental comparison and preliminary results. *Magnetic resonance in medicine.* 1996;36(5):726—736.

9. Forkert ND, Fiehler J, Ries T, *et al.* Reference-based linear curve fitting for bolus arrival time estimation in 4D MRA and MR perfusion-weighted image sequences. *Magnetic Resonance in Medicine.* 2011;65(1):289-294.

10. Fan S, Bian Y, Wang E, *et al.* An Automatic Estimation of Arterial Input Function Based on Multi-Stream 3D CNN. *Frontiers in Neuroinformatics.* 2019;13:49.

11. Straka M, Albers G, Bammer R. Real-Time Diffusion-Perfusion Mismatch Analysis in Acute Stroke. *Journal of magnetic resonance imaging : JMRI.* 2010;32:1024-37.

12. Mouridsen K, Christensen S, Gyldensted L, Østergaard L. Automatic selection of arterial input function using cluster analysis. *Magnetic Resonance in Medicine.* 2006;55(3):524-531.

13. Sorensen AG, Copen WA, Østergaard L, *et al.* Hyperacute Stroke: Simultaneous Measurement of Relative Cerebral Blood Volume, Relative Cerebral Blood Flow, and Mean Tissue Transit Time. *Radiology.* 1999;210(2):519-527. PMID: 10207439.

14. Mouannes-Srour J, Shin W, Ansari S, *et al.* Correction for arterial-tissue delay and dispersion in absolute quantitative cerebral perfusion DSC MR imaging. *Magnetic Resonance in Medicine.* 2012;68(2):495–506.

15. Lorenz C, Benner T, Chen PJ, *et al.* Automated perfusion-weighted MRI using localized arterial input functions. *Journal of Magnetic Resonance Imaging.* 2006;24(5):1133-1139.

16. Condat L. Discrete Total Variation: New Definition and Minimization. *SIAM Journal on Imaging Sciences.* 2017;10(3):1258-1290.

17. Roberts M, Chen K, Irion KL. A Convex Geodesic Selective Model for Image Segmentation. *J. Math. Imaging Vis..* 2019;61(4):482–503.

18. Chan T, Vese L. Active contours without edges. *IEEE Transactions on Image Processing.* 2001;10(2):266-277.

19. Badshah N, Chen K. Image selective segmentation under geometrical constraints using an active contour approach. *Communications in Computational Physics.* 2009;7:759-778.

20. Brown ES, Chan T, Bresson X. Completely Convex Formulation of the Chan-Vese Image Segmentation Model. *International Journal of Computer Vision.* 2011;98:103-121.

21. Weickert J, Romeny B, Viergever M. Efficient and reliable schemes for nonlinear diffusion filtering. *IEEE Transactions on Image Processing.* 1998;7(3):398-410.

22. Tang M, Chen T, Zhang X, Huang X. GRE T2* -weighted MRI: Principles and clinical applications. *BioMed research international.* 2014;2014:312142.

23. Calamante F, Mørup M, Hansen LK. Defining a local arterial input function for perfusion MRI using independent component analysis. *Magnetic Resonance in Medicine.* 2004;52(4):789-797.

24. Yang F, Bal SSB, Sung YF, Peng GS. Mathematical Framework of Deconvolution Algorithms for Quantification of Perfusion Parameters. *Acta neurologica Taiwanica.* 2020;29(3):79—85.

25. Bal SS, Yang FPG, Sung YF, Chen K, Yin JH, Peng GS. Optimal Scaling Approaches for Perfusion MRI with Distorted Arterial Input Function (AIF) in Patients with Ischemic Stroke. *Brain Sciences.* 2022;12(1).

26. Wu O, Østergaard L, Koroshetz WJ, *et al.* Effects of tracer arrival time on flow estimates in MR perfusion-weighted imaging. *Magnetic Resonance in Medicine.* 2003;50(4):856-864.

27. Smith M, Lu H, Trochet S, Frayne R. Removing the effect of SVD algorithmic artifacts present in quantitative MR perfusion studies. *Magnetic Resonance in Medicine.* 2004;51(3):631-634.

28. A Reformulated Convex and Selective Variational Image Segmentation Model and Its Fast Multilevel Algorithm. *Numerical Mathematics: Theory, Methods and Applications.* 2018;12(2):403–437.

29. Spencer JA, Chen K. A CONVEX AND SELECTIVE VARIATIONAL MODEL FOR IMAGE SEGMENTATION. *Communications in Mathematical Sciences.* 2015;13:1453-1472.

30. Winder A, d'Esterre CD, Menon BK, Fiehler J, Forkert ND. Automatic arterial input function selection in CT and MR perfusion datasets using deep convolutional neural networks. *Medical Physics.* 2020;47(9):4199-4211.

31. Arioz U, Oguz K, Baysal U, Cila A. Multislice Brain Mapping and Quantification of Perfusion MRI Data. in *Conference Proceedings. 2nd International IEEE EMBS Conference on Neural Engineering, 2005.*:9-12 2005.

32. Ramos-Cabrer P, Campos F, Sobrino T, Castillo J. Targeting the Ischemic Penumbra. *Stroke.* 2011;42(1_suppl_1):S7-S11.

33. Kasam M. SU-E-E-05: The Role of Conventional MR Physics, Resting State Functional MR Physics and MR Spectroscopy for the In-Situ Monitoring of Infarct and Peri-Infarct Tissue and for the Precise Diagnosis of Acute Ischemic Stroke. *Medical Physics.* 2013;40(6Part4):118-118.

34. Chen JJ, Smith MR, Frayne R. The impact of partial-volume effects in dynamic susceptibility contrast magnetic resonance perfusion imaging. *Journal of Magnetic Resonance Imaging.* 2005;22(3):390-399.

35. Campbell BC, Christensen S, Levi CR, *et al.* Comparison of Computed Tomography Perfusion and Magnetic Resonance Imaging Perfusion-Diffusion Mismatch in Ischemic Stroke. *Stroke.* 2012;43(10):2648-2653.

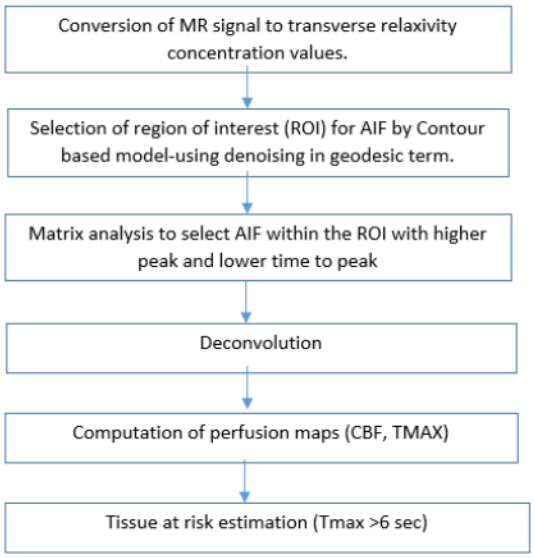

Figure 1: Model Pipeline used to estimate perfusion parameters after extracting AIF by a contour based geodesic model.

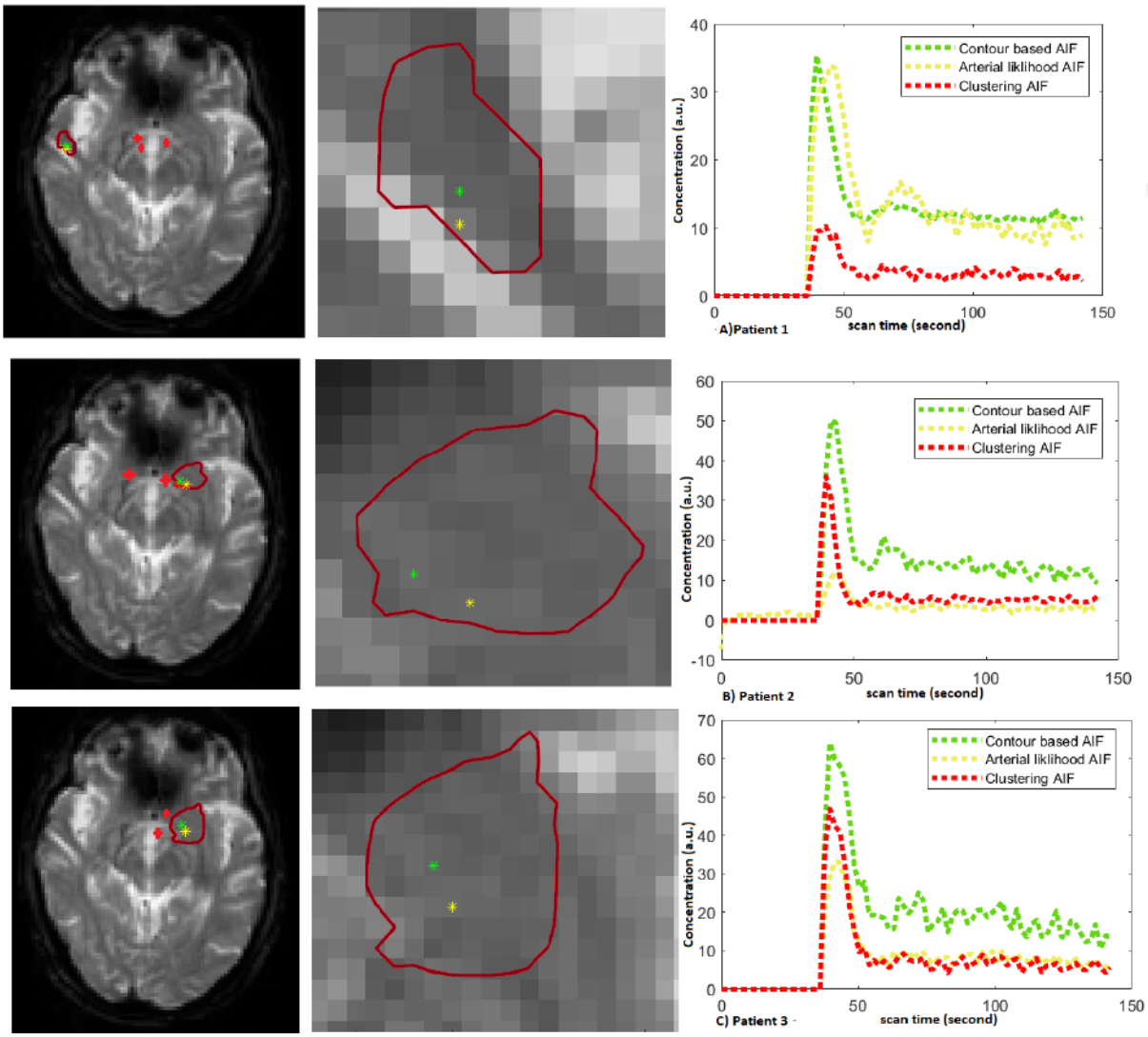

Figure 2: AIF voxels selected by the contour based AIF (green), arterial likelihood selection method (yellow) and clustering method (red) (left column) (b) Zoomed in images of contour (dark red) used for AIF selection demonstrates that the voxels selected for contour based AIF (green), arterial likelihood selection method (yellow) were very close to each other. (central column) (c) Concentration curves of the selected AIF voxels (Right column). contour based AIF segmentation method (green curve) selects AIF curve with larger amplitude or higher peak position, and fast attenuation represented by early time to peak or positive Δ center than the latter two methods. Each row demonstrates different patient

.

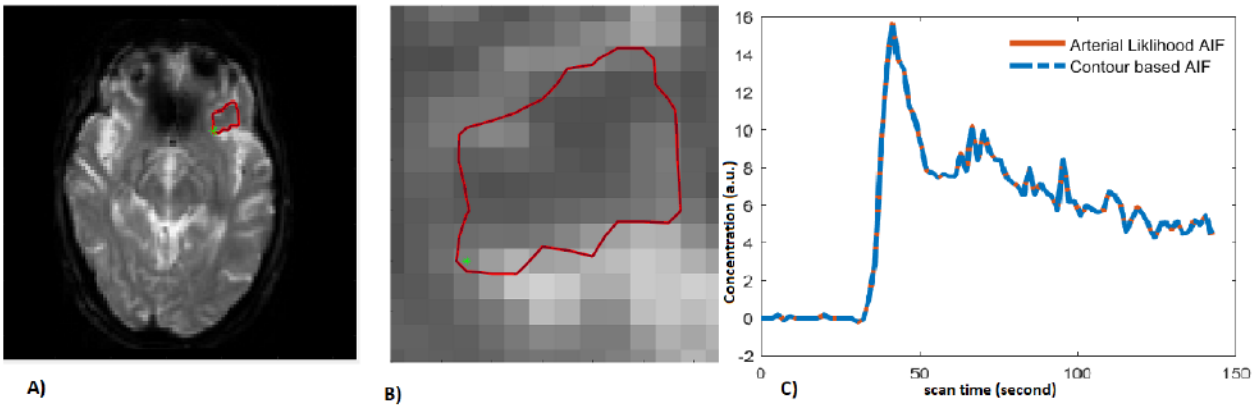

Figure 3: Similar AIF voxel (Green) selected by the contour based AIF and arterial likelihood selection method (left column) (b) Zoomed in images of contour (dark red) used for AIF selection demonstrates similar voxel selected for contour based AIF (green) and arterial likelihood selection method (central column). (c) AIF Concentration curves of the selected AIF voxel (right column).

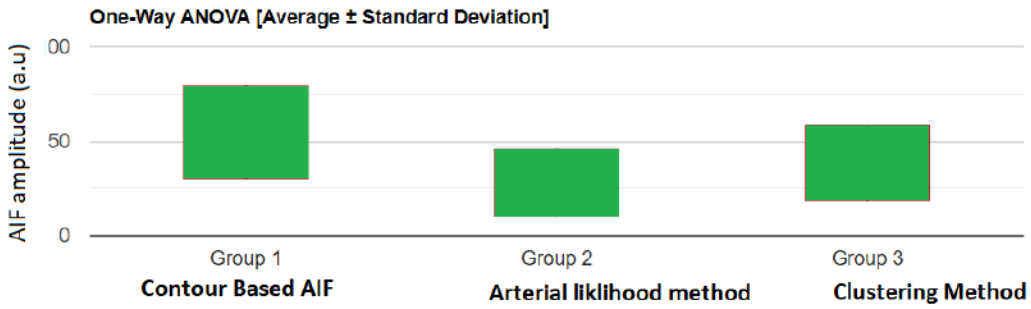

Figure 4: Comparison of AIF amplitude for the AIF selected by the three methods in the patient cohort. A one-way ANOVA revealed that there was a statistically significant difference in AIF amplitude (peak) between the three AIF selection methods (F value = 5.66 , P value = .0067).

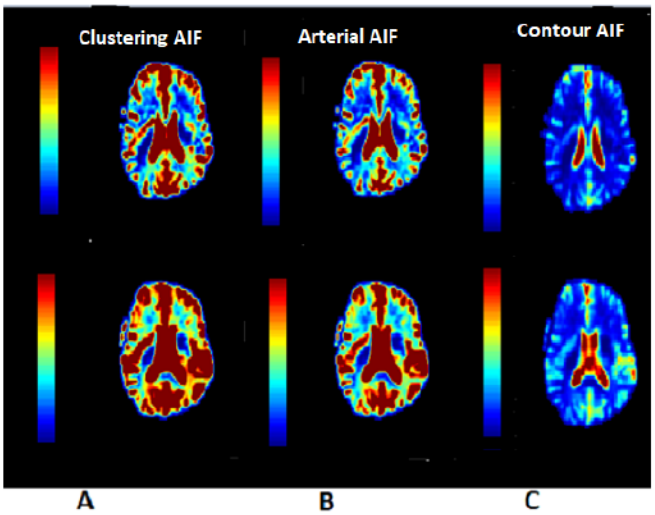

Figure 5: CBF maps estimated by AIF from (A) clustering (B) arterial likelihood method and (C) contour based AIF from left to right. CBF values obtained from the contour based AIF method are lower than the latter two methods due to the larger peak and lower time to peak of the AIF. This allows to locate the core regions with decreased blood flow more precisely and accurately.

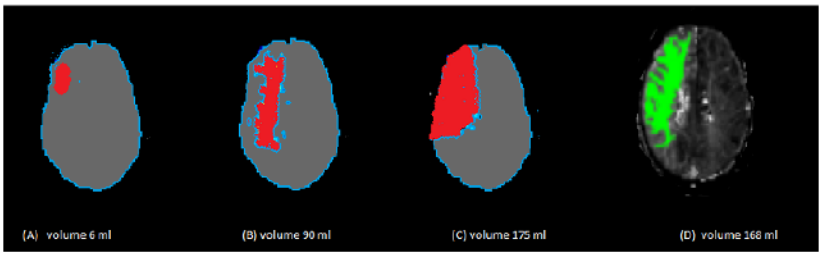

Figure 6: Tissue at risk (Red) maps estimated by AIF from (A) clustering (B) arterial likelihood method and (C) contour based AIF from left to right. (D) Tissue at risk identified by the commercial software. Tissue at risk is identified by Tmax> 6 sec and is overlaid on brain masks. Among the three methods, contour based AIF method has the closest prediction of Tissue at risk (168 mL) with the tissue at risk identified by the commercial software (175 mL) considered as golden standard for perfusion processing outcome.

Table 1: The difference of curve characteristics between the arterial liklihood method and contour based peak height AIF selection method.

Sample	amplitude (a.u)			center (s)			Correlation
	Contour based AIF	Arterial likelihood	Δamplitude (a.u)	Arterial likelihood	Contour based AIF	Δcenter (s)	
1	29	21	8	41.4	39.6	1.8	0.8
2	41.4	41.4	0	17.7	17.7	0	1
3	90.8	27	63.8	27	27	0	0.8
4	46	20	26	43.2	41.4	1.8	0.6
5	80.6	64.3	16.3	33.9	37.5	-3.6	0.8
6	12	4.3	7.7	50.4	45	5.4	0.7
7	36	19.6	16.4	48.6	46.8	1.8	0.9
8	59.7	13.2	46.5	43.2	45	-1.8	0.7
9	39.5	33.7	5.8	45	43.2	1.8	0.9
10	50.1	12.2	37.9	43.2	41.4	1.8	0.9
11	53.8	33.7	20.1	41.4	41.4	0	0.9
12	69.7	64.1	5.6	39.6	37.8	1.8	0.8
13	42.5	16.1	26.4	34.2	34.2	0	0.9
14	109.5	42.8	66.7	36	37.8	-1.8	0.7
15	56.5	10.8	45.7	41.4	36	5.4	0.8

Table 2: The difference of curve characteristics between the clustering method and contour based peak height AIF selection method.

Sample	amplitude (a.u)			center (s)			Correlation
	Contour based AIF	Clustering method	Δ amplitude (a.u)	Clustering method	Contour based AIF	Δcenter (s)	
1	29	3.4	25.6	41.4	39.6	1.8	0.8
2	41.4	29.8	11.6	19.5	17.7	1.8	0.8
3	90.8	45.7	45.1	30.6	27	3.6	0.2
4	46	36	10	41.4	41.4	0	0.8
5	80.6	65.2	15.4	37.8	37.8	0	0.8
6	12	60.1	-48.1	50.4	45	5.4	0.7
7	36	61.7	-25.7	50.4	46.8	3.6	0.9
8	59.7	48.9	10.8	39.6	45	-5.4	0.7
9	39.5	10.2	29.3	43.2	43.2	0	0.9
10	50.11	36	14.11	39.6	41.4	-1.8	0.9
11	53.8	46.7	7.1	39.6	41.4	-1.8	0.9
12	69.7	64.1	5.6	41.4	37.8	3.6	0.8
13	42.5	16.1	26.4	36	34.2	1.8	0.8
14	109.5	42.8	66.7	37.8	37.8	0	0.7
15	56.5	10.8	45.7	39.6	36	3.6	0.8

Table 3: Group mean difference between the Contour based peak height AIF method and the previous AIF selection methods.

Method	amplitude (a.u)	center (s)	Correlation coefficient
Clustering method	16.7	1.08	0.7
Arterial likelihood method	26.1	0.9	0.8

Table 4: Perfusion parameters (Tmax and CBF) for different AIF selection methods.

Method		Tmax (s)	CBF (a.u)
Contour Based AIF	Mean	1.87	81.9
	SD	2.09	64.7
Arterial Likelihood method	Mean	1.6	178.3
	SD	3.01	139.9
Clustering method	Mean	1.13	296.5
	SD	2.8	229.6

515

516 **Figure legends**

517

518 Figure 1 : Model Pipeline used to estimate perfusion parameters after extracting AIF by a
519 contour based geodesic model.

520

521 Figure 2: AIF voxels selected by the contour based AIF (green), arterial likelihood selection
522 method (yellow) and clustering method (red) (left column) (b) Zoomed in images of contour
523 (dark red) used for AIF selection demonstrates that the voxels selected for contour based AIF
524 (green), arterial likelihood selection method (yellow) were very close to each other. (central
525 column) (c) Concentration curves of the selected AIF voxels (Right column). contour based
526 AIF segmentation method (green curve) selects AIF curve with larger amplitude or higher
527 peak position, and fast attenuation represented by early time to peak or positive Δ center
528 than the latter two methods. Each row demonstrates different patient

529

530 Figure 3: Similar AIF voxel (Green) selected by the contour based AIF and arterial likeli-
531 hood selection method (left column) (b) Zoomed in images of contour (dark red) used for
532 AIF selection demonstrates similar voxel selected for contour based AIF (green) and arterial
533 likelihood selection method (central column). (c) AIF Concentration curves of the selected
534 AIF voxel (right column).

535

536 Figure 4: Comparison of AIF amplitude for the AIF selected by the three methods in the
537 patient cohort. A one-way ANOVA revealed that there was a statistically significant differ-
538 ence in AIF amplitude (peak) between the three AIF selection methods (F value = 5.66 ,
539 P value = .0067).

540

541 Figure 5: CBF maps estimated by AIF from (A) clustering (B) arterial likelihood method
542 and (C) contour based AIF from left to right. CBF values obtained from the contour based
543 AIF method are lower than the latter two methods due to the larger peak and lower time
544 to peak of the AIF. This allows to locate the core regions with decreased blood flow more

545 precisely and accurately.

546

547 Figure 6: Tissue at risk (Red) maps estimated by AIF from (A) clustering (B) arterial likeli-
548 hood method and (C) contour based AIF from left to right. (D) Tissue at risk identified by
549 the commercial software. Tissue at risk is identified by Tmax> 6 sec and is overlaid on brain
550 masks. Among the three methods, contour based AIF method has the closest prediction of
551 Tissue at risk (168 mL) with the tissue at risk identified by the commercial software (175
552 mL) considered as golden standard for perfusion processing outcome.

553